Hypernuclei in the deformed Skyrme-Hartree-Fock approach

Xian-Rong Zhou,[1] H.-J. Schulze,[2] H. Sagawa,[3] Chen-Xu Wu,[1] and En-Guang Zhao[4]
[1] *Department of Physics and Institute of Theoretical Physics and Astrophysics, Xiamen University, Xiamen 361005, People's Republic of China*
[2] *INFN Sezione di Catania, Via Santa Sofia 64, I-95123 Catania, Italy*
[3] *Center for Mathematical Sciences, University of Aizu, Aizu-Wakamatsu, Fukushima 965-8560, Japan*
[4] *Institute of Theoretical Physics, Chinese Academy of Sciences, Beijing 100080, People's Republic of China*
(Received 11 May 2007; published 11 September 2007)

The properties of Λ hypernuclei in a broad mass region are studied by using a deformed Hartree-Fock approach using realistic nucleonic Skyrme forces, pairing correlations, and a microscopically determined lambda-nucleon interaction based on Brueckner-Hartree-Fock calculations of hypernuclear matter. The results suggest that the core nuclei and the corresponding hypernuclei have similar deformations with the same sign. Some light single-Λ hypernuclei are substantially deformed and the Λ binding energy is modified by the deformation.

DOI: 10.1103/PhysRevC.76.034312 PACS number(s): 21.80.+a, 21.65.+f, 21.10.Dr, 21.30.Fe

I. INTRODUCTION

The study of hypernuclei is crucial for providing information about hyperon-nucleon (YN) and hyperon-hyperon (YY) interactions. Quantitative information on these forces is very important to understand the properties of multistrange systems and also neutron stars. The experimental study of hypernuclei [1–5] is one of the few possibilities to constrain theoretical models of these interactions. Currently there are many experimental data for various single-Λ hypernuclei over almost the whole mass table [5] and a few double-Λ hypernuclei [6–9].

Many theoretical studies of hypernuclei have been performed either based on phenomenological models, i.e., relativistic mean-field models [10–12], Skyrme Hartree-Fock (SHF) models [13], or Woods-Saxon potential [14] with an effective hyperon-nucleon interaction, or by using microscopically derived lambda-nucleon (ΛN) forces. In Refs. [15,16] the properties of Λ-hypernuclei were studied by using a ΛN G-matrix that incorporates the short-range correlations, whereas in Refs. [17,18] a SHF model was used together with a microscopical ΛN force without adjustable parameters, derived from Brueckner-Hartree-Fock (BHF) calculations of isospin-symmetric hypernuclear matter [19].

All these calculations of hypernuclei were based on spherical symmetry, except some attempts of deformed HF calculations with nonrealistic interactions [20] and the Nilsson model study of p-shell nuclei in Ref. [21]. However, it is well known that many p-shell and d-shell nuclei are deformed in the ground state. For example, according to experiment, ^{10}B and ^{11}C have large quadrupole moments [22]. One can describe deformed (hyper)nuclei within several models such as the α-cluster model [2], the projected shell model [23], and the deformed self-consistent SHF method [24]. Deformation of p-shell hypernuclei was taken into account in Ref. [21] by using the Nilsson model [25,26] and assuming the same deformation for both the core and the hypernuclei. So far there is no study of a self-consistent model treating the core and the hypernuclei with realistic effective interactions for both nucleon-nucleon and ΛN channels.

The aim of this article is to investigate how much the observables of hypernuclei depend on the deformation in a deformed SHF (DSHF) model, including the hyperon degree of freedom (hereafter we call this model the extended DSHF model). The DSHF method has been used to describe the properties of light and medium-heavy normal nuclei in Ref. [27] and is extended in this article to the study of hypernuclei. For this purpose we generalize the microscopic ΛN force developed in Refs. [17,18] for nearly symmetric nuclei to isospin-asymmetric nuclei. This effective ΛN interaction is derived from Brueckner-Hartree-Fock calculations of isospin-asymmetric hypernuclear matter [19] with the Nijmegen soft-core hyperon-nucleon potential NSC89 [28] and the Argonne V_{18} nucleon-nucleon interaction [29], including explicitly the coupling of the lambda-nucleon to the sigma-nucleon states. Furthermore, nucleonic pairing correlations are now included in the model and we perform the DSHF and extended DSHF calculations using three different nucleonic Skyrme forces.

The present study is a generalization of the calculations of closed-shell spherical hypernuclei in Refs. [17,18] for more complex open-shell nuclei using realistic effective interactions. We study many nuclei in a broad region of the mass table from light p- and sd-shell nuclei, medium mass nuclei, and also heavy nuclei up to ^{207}Pb and $^{208}_{\Lambda}$Pb.

This article is organized as follows. In Sec. II we present the SHF formalism including an effective hyperon-nucleon interaction derived from microscopic BHF calculations of asymmetric nuclear matter. The calculated results of DSHF for core nuclei and extended DSHF for hypernuclei with one or two Λ are given in Sec. III and compared with the experimental data. Finally, discussions and conclusions are given in Sec. IV.

II. FORMALISM

Our model is based on the self-consistent DSHF method [24] solved in coordinate space with axially symmetric shape [30], including the ΛN interaction. The total energy of a hypernucleus in the extended DSHF model is expressed as

$$E = \int \mathrm{d}^3\boldsymbol{r}\,\varepsilon(\boldsymbol{r}) \tag{1}$$

with the energy density functional

$$\varepsilon = \varepsilon_N[\rho_n, \rho_p, \tau_n, \tau_p, \boldsymbol{J}_n, \boldsymbol{J}_p] + \varepsilon_\Lambda[\rho_n, \rho_p, \rho_\Lambda, \tau_\Lambda], \quad (2)$$

where ε_N is the total energy density of neutrons and protons [24,31] and ε_Λ is the contribution due to the presence of hyperons. The one-body density ρ_q, kinetic density τ_q, and spin-orbit current $\boldsymbol{J}_q$ read

$$\rho_q = \sum_{i=1}^{N_q} n_q^i \left|\phi_q^i\right|^2, \quad (3a)$$

$$\tau_q = \sum_{i=1}^{N_q} n_q^i \left|\nabla\phi_q^i\right|^2, \quad (3b)$$

$$\boldsymbol{J}_q = \sum_{i=1}^{N_q} n_q^i \phi_q^{i\,*} \left(\nabla\phi_q^i \times \boldsymbol{\sigma}\right)/i, \quad (3c)$$

where ϕ_q^i $(i = 1, N_q)$ are the single-particle wave functions of the N_q occupied states for the different particles $q = n, p, \Lambda$.

The occupation probabilities n_q^i (for nucleons only) are calculated by taking into account pairing interactions within a BCS approximation. The pairing interaction is taken to be a density-dependent delta force [32],

$$V_q(\boldsymbol{r}_1, \boldsymbol{r}_2) = V_q' \left[1 - \frac{\rho_N(r)}{\rho_0}\right] \delta(\boldsymbol{r}_1 - \boldsymbol{r}_2), \quad (4)$$

where $\rho_N(r)$ is the nucleonic HF density at $\boldsymbol{r} = (\boldsymbol{r}_1 + \boldsymbol{r}_2)/2$ and $\rho_0 = 0.16\,\mathrm{fm}^{-3}$. As pairing strength we use $V_q' = -410\,\mathrm{MeVfm}^3$ for both neutrons and protons of light nuclei [33] and $V_p' = -1146\,\mathrm{MeVfm}^3$, $V_n' = -999\,\mathrm{MeVfm}^3$ for medium-mass and heavy nuclei. A smooth energy cutoff is employed in the BCS calculations [34]. In the case of an odd number of nucleons, the orbit occupied by the unpaired nucleon is blocked in the BCS calculations, as described in Ref. [26].

For the nucleonic energy density functional ε_N we use the standard Skyrme forces SIII, SkI4, or SGII, whereas the energy-density functional due to the presence of hyperons, ε_Λ, is written as [17],

$$\varepsilon_\Lambda = \frac{\tau_\Lambda}{2m_\Lambda} + \varepsilon_{N\Lambda}(\rho_n, \rho_p, \rho_\Lambda) + \left(\frac{m_\Lambda}{m_\Lambda^*(\rho_n, \rho_p, \rho_\Lambda)} - 1\right) \frac{\tau_\Lambda - C\rho_\Lambda^{5/3}}{2m_\Lambda} \quad (5)$$

with $C = (3/5)(3\pi^2)^{2/3} \approx 5.742$ and

$$\varepsilon_{N\Lambda} = (\rho_n + \rho_p + \rho_\Lambda)\frac{B}{A}(\rho_n, \rho_p, \rho_\Lambda) - (\rho_n + \rho_p)\frac{B}{A}(\rho_n, \rho_p, 0) - \frac{C\rho_\Lambda^{5/3}}{2m_\Lambda}. \quad (6)$$

The energy density functional $\varepsilon_{N\Lambda}$ is obtained from a fit to the binding energy per baryon, $B/A(\rho_n, \rho_p, \rho_\Lambda)$, of asymmetric hypermatter, as generated by BHF calculations [19]. The adequate Λ effective mass,

$$\frac{m_\Lambda^*}{m_\Lambda} = \left[1 + \frac{U_\Lambda\left(k_F^{(\Lambda)}\right) - U_\Lambda(0)}{k_F^{(\Lambda)2}/2m_\Lambda}\right]^{-1}, \quad (7)$$

is computed from the BHF single-particle potentials $U_\Lambda(k)$ obtained in the same calculations. In practice we use the following parametrizations of energy density and Λ effective mass in terms of the partial densities $\rho_n, \rho_p, \rho_\Lambda$ (ρ_N and ρ_Λ given in units of fm^{-3}, $\varepsilon_{N\Lambda}$ in $\mathrm{MeV\,fm}^{-3}$):

$$\varepsilon_{N\Lambda} \approx -\left[368 - (1717 + 268\alpha - 920\alpha^2)\rho_N + (2932 - 776\alpha + 2483\alpha^2)\rho_N^2\right]\rho_N\rho_\Lambda + \left(449 - 2470\rho_N + 5834\rho_N^2\right)\rho_N\rho_\Lambda^{5/3}, \quad (8)$$

$$\frac{m_\Lambda^*}{m_\Lambda} \approx 1 - (1.58 + 0.12\alpha - 0.12\alpha^2 + 0.54y - 0.14y^2)\rho_N + (4.11 + 2.11\alpha + 2.88\alpha^2 + 0.35y + 1.17y^2)\rho_N^2 - (4.03 + 7.08\alpha + 5.18\alpha^2 - 0.93y + 3.27y^2)\rho_N^3, \quad (9)$$

where $\rho_N = \rho_n + \rho_p$, $\alpha = (\rho_n - \rho_p)/\rho_N$, and $y = \rho_\Lambda/\rho_N$.

The minimization of the total energy Eq. (1) implies the SHF Schrödinger equation

$$\left[-\nabla \cdot \frac{1}{2m_q^*(\boldsymbol{r})}\nabla + V_q(\boldsymbol{r}) - i\nabla W_q(\boldsymbol{r}) \cdot (\nabla \times \boldsymbol{\sigma})\right]\phi_q^i(\boldsymbol{r}) = e_q^i \phi_q^i(\boldsymbol{r}) \quad (10)$$

and the gap equation

$$n_q^i = \frac{1}{2}\left[1 - \frac{e_q^i - \mu_q}{\sqrt{\left(e_q^i - \mu_q\right)^2 + \left(f_q^i \Delta_q^i\right)^2}}\right], \quad (11)$$

$$\Delta_q^i = -\sum_k (fuv)_q^k \int d^3\boldsymbol{r}_1 d^3\boldsymbol{r}_2 \left|\phi_q^k(\boldsymbol{r}_1)\right|^2 V_q(\boldsymbol{r}_1, \boldsymbol{r}_2) \left|\phi_q^i(\boldsymbol{r}_2)\right|^2 \quad (12)$$

with the single-particle energies e_q^i, the chemical potentials μ_q, $(uv)_q^k = \sqrt{n_q^k(1 - n_q^k)}$, and the additional factors f_q^k due to the smooth energy-dependent pairing cutoff procedure [34]. The extended SHF mean fields in Eq. (10) are given by

$$V_q = V_q^{\mathrm{SHF}} + \frac{\partial\varepsilon_{N\Lambda}}{\partial\rho_q} + \frac{\partial}{\partial\rho_q}\left(\frac{m_\Lambda}{m_\Lambda^*}\right)\frac{\tau_\Lambda - C\rho_\Lambda^{5/3}}{2m_\Lambda},$$

$$V_\Lambda = \frac{\partial\varepsilon_{N\Lambda}}{\partial\rho_\Lambda} + \frac{\partial}{\partial\rho_\Lambda}\left(\frac{m_\Lambda}{m_\Lambda^*}\right)\frac{\tau_\Lambda - C\rho_\Lambda^{5/3}}{2m_\Lambda} - \left(\frac{m_\Lambda}{m_\Lambda^*} - 1\right)\frac{5}{3}\frac{C\rho_\Lambda^{2/3}}{2m_\Lambda}, \quad (13)$$

where $V_q^{\mathrm{SHF}}(q = n, p)$ is the nucleonic Skyrme mean field without hyperons and W_q is the nucleonic spin-orbit mean field, as given in Refs. [24,31]. At the present level of approximation we do not include a spin-orbit force for Λ, which is justified by the experimental observation of very small spin-orbit splittings [35]. The total nucleon mean field is thus modified due to the presence of hyperons, causing a rearrangement of the nucleonic core of a hypernucleus.

Axial symmetry is assumed for the SHF deformed potentials and the Schrödinger equation is solved in cylindrical

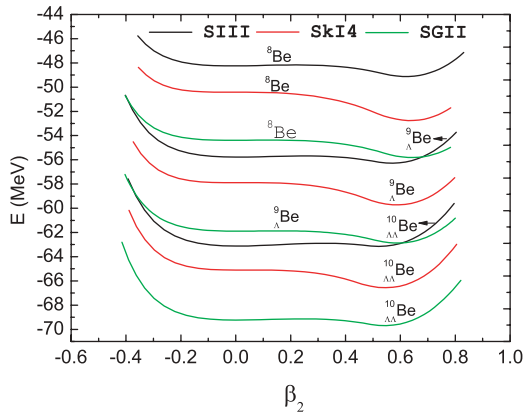

FIG. 1. (Color online) Self-consistent DSHF calculations of ^{8}Be, $^{9}_{\Lambda}$Be, and $^{10}_{\Lambda\Lambda}$Be with different interactions SIII, SkI4, and SGII.

coordinates (r, z). The optimal quadrupole deformation parameters

$$\beta_2^{(q)} = \sqrt{\frac{\pi}{5}}\frac{\langle 2z^2 - r^2\rangle_q}{\langle z^2 + r^2\rangle_q} \tag{14}$$

are found by minimizing the total energy of the (hyper) nucleus.

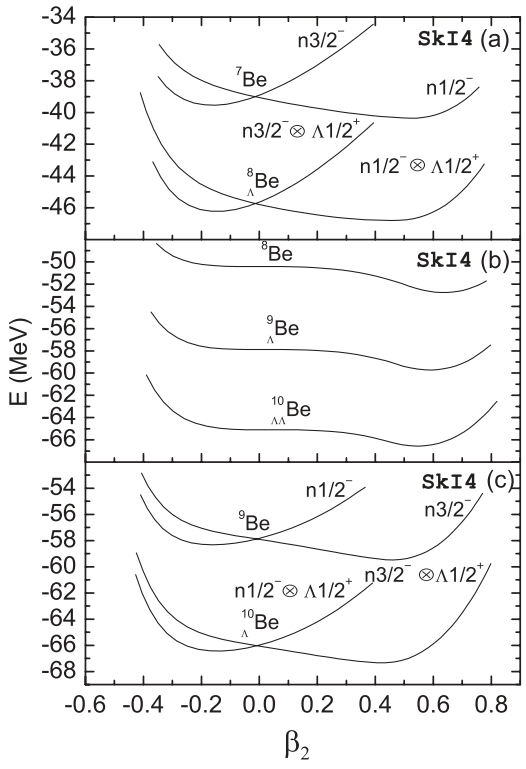

FIG. 2. Self-consistent DSHF calculations with the SkI4 interaction for (a) ^{7}Be and $^{8}_{\Lambda}$Be; (b) ^{8}Be, $^{9}_{\Lambda}$Be, and $^{10}_{\Lambda\Lambda}$Be; and (c) ^{9}Be and $^{10}_{\Lambda}$Be. Each single-particle and single-Λ configuration is assigned by the quantum number K^{π} in the deformed potential. The abbreviation "n" stands for the neutron configuration.

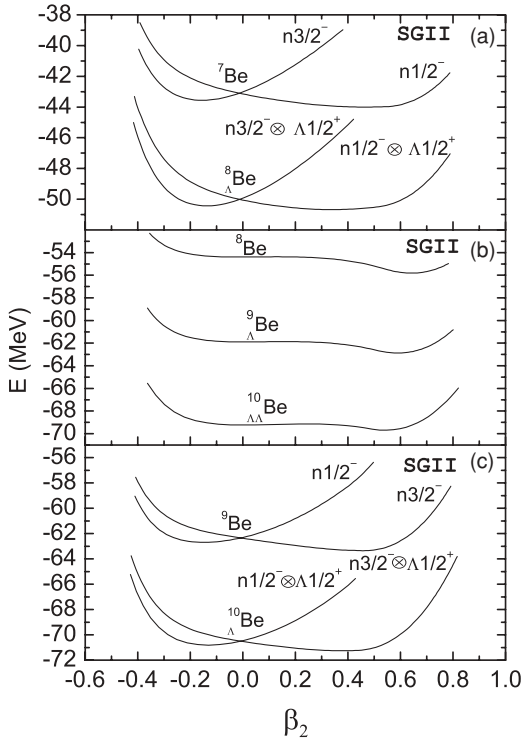

FIG. 3. Same as described in the caption to Fig. 2 but for the SGII interaction.

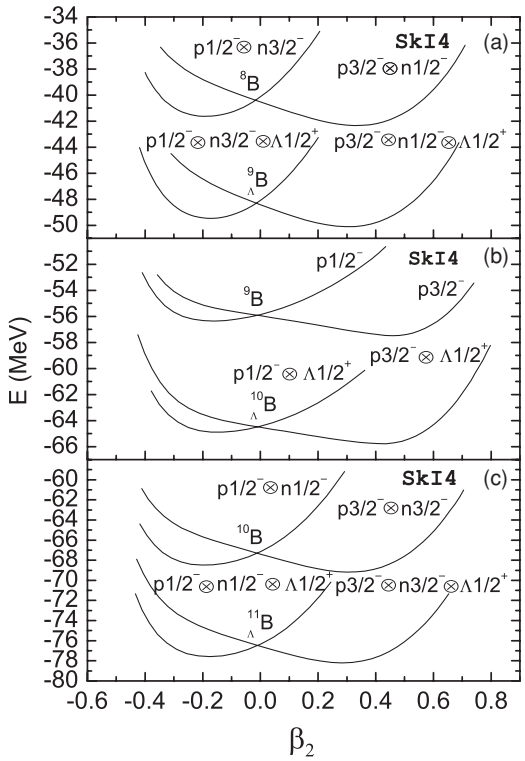

FIG. 4. Self-consistent DSHF calculations with the SkI4 interaction for (a) ^{8}B and $^{9}_{\Lambda}$B, (b) ^{9}B and $^{10}_{\Lambda}$B, and (c) ^{10}B and $^{11}_{\Lambda}$B. The abbreviation "p" stands for the proton configuration. See the caption to Fig. 2 for more details.

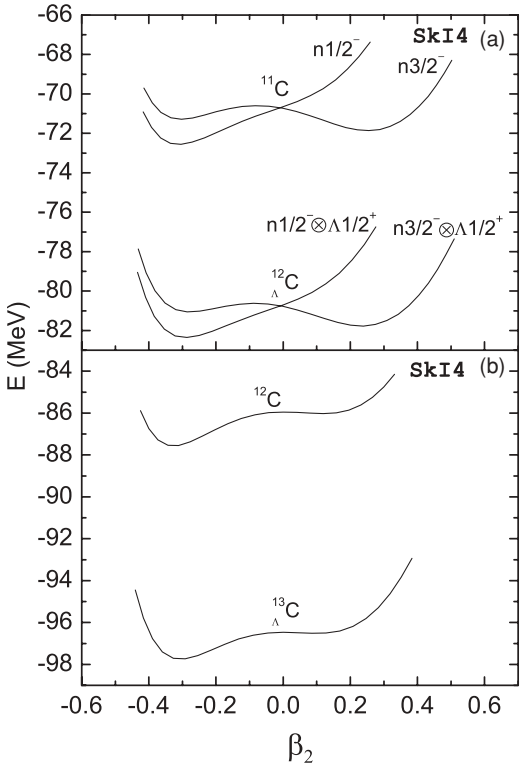

FIG. 5. Self-consistent DSHF calculations with the SkI4 interaction for (a) ^{11}C and $^{12}_{\Lambda}$C and (b) ^{12}C and $^{13}_{\Lambda}$C. See the caption to Fig. 2 for more details.

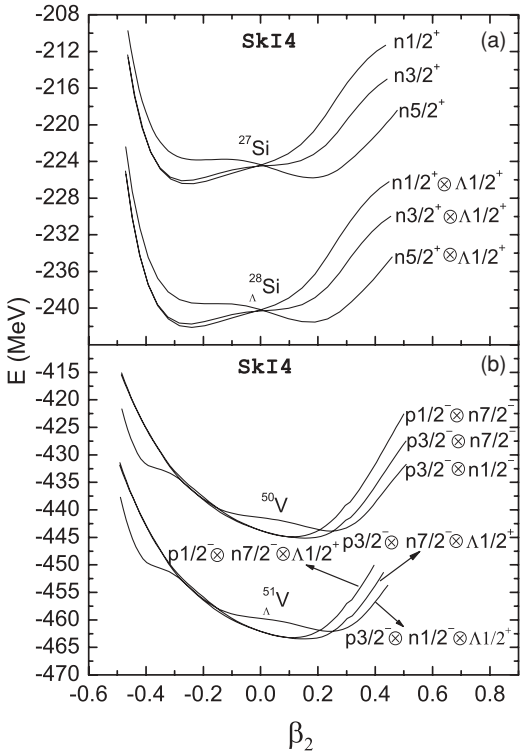

FIG. 6. Self-consistent DSHF calculations with the SkI4 interaction for (a) ^{27}Si and $^{28}_{\Lambda}$Si and (b) ^{50}V and $^{51}_{\Lambda}$V. See the captions to Figs. 2 and 4 for more details.

III. RESULTS

We calculate the various experimentally studied hypernuclei including light, medium, and heavy systems by performing the DSHF+BCS and extended DSHF+BCS calculations with the microscopic ΛN force. In order to obtain realistic deformation minima for C isotopes and C hypernuclei, we reduce the spin-orbit interactions of the SkI4 and SGII forces to 60% of the original strength as in Ref. [27], while the original strength is used in all other HF and extended HF calculations of nuclei and hypernuclei, respectively. Several hypernuclei turn out to be spherical or nearly spherical in the present DSHF model, while some p-shell and sd-shell hypernuclei show deformed minima in the calculated energy surfaces. We will discuss in the following the effect of deformations on hypernuclei.

The nucleus ^{8}Be is known to be strongly deformed due to its double-α structure. In order to study the interaction dependence of the results, we display in Fig. 1 the energy surfaces for ^{8}Be and the hypernuclei $^{9}_{\Lambda}$Be and $^{10}_{\Lambda\Lambda}$Be, obtained with the three different Skyrme forces SIII, SkI4, and SGII. These interactions are commonly used in mean-field calculations and also random phase approximations for excited states. While the total energies predicted by the different forces vary by about 8 MeV in Fig. 1, the Λ binding energy,

$$B_\Lambda = E(^{A-1}Z) - E(^{A}_{\Lambda}Z), \tag{15}$$

and the $\Lambda\Lambda$ bond energy,

$$\Delta B_{\Lambda\Lambda} = 2E(^{A-1}_{\Lambda}Z) - E(^{A-2}Z) - E(^{A}_{\Lambda\Lambda}Z), \tag{16}$$

are nearly the same with the three forces, namely we obtain $B_\Lambda = 7.16, 6.96, 7.06$ MeV and $\Delta B_{\Lambda\Lambda} = -0.29, -0.12, -0.24$ MeV with the SIII, SkI4, and SGII force, respectively, compared with the experimental values of $B_\Lambda = 6.71 \pm 0.04$ MeV [3] or 5.99 ± 0.07 MeV [5], and $\Delta B_{\Lambda\Lambda} = 4.3 \pm 0.4$ MeV [6] or -4.9 ± 0.7 MeV [7].

The relativistic mean-field model of Ref. [11] predicts $\Delta B_{\Lambda\Lambda} \approx 0.3$ MeV for this nucleus. Although there are two experimental reports about the double-Λ hypernucleus $^{10}_{\Lambda\Lambda}$Be, more experimental events are desperately needed to confirm the data with better statistics, as discussed in Ref. [8]. In fact a recent measurement of $^{6}_{\Lambda\Lambda}$He shows a weakly attractive $\Delta B_{\Lambda\Lambda} \approx +1$MeV for this nucleus [9]. We remark that the slightly repulsive bond energy is obtained because of no $\Lambda\Lambda$ interaction in our model, because the underlying NSC89 potential [28] does not provide it. Results obtained with the NSC97 potentials including hyperon-hyperon interactions yield similarly small numbers, however [18,36].

The predicted deformations are very similar for the three interactions, namely $\beta_2 = 0.63, 0.63, 0.65$ for ^{8}Be, $\beta_2 = 0.57, 0.59, 0.59$ for $^{9}_{\Lambda}$Be, and $\beta_2 = 0.52, 0.55, 0.55$ for $^{10}_{\Lambda\Lambda}$Be, respectively. The calculations with the three interactions suggest that the core nucleus ^{8}Be and the $^{9}_{\Lambda}$Be, $^{10}_{\Lambda\Lambda}$Be hypernuclei have similar deformation parameters with the same sign, which agree with the results of Ref. [2]. These results also justify the assumption of the same deformations in the core and the hypernuclei made in the Nilsson model potential [21]. For comparison, we perform also spherical HF calculations for the same nuclei disregarding the deformation. The predicted

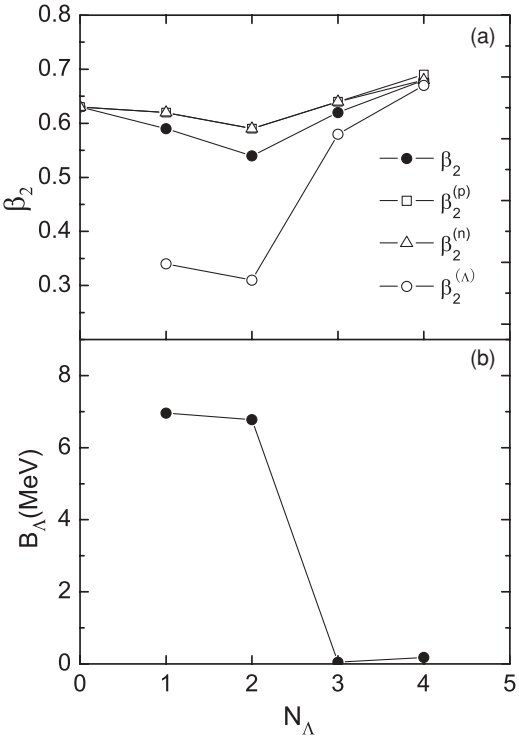

FIG. 7. Deformation parameters (upper panel) and binding energies of the last Λ (lower panel) for multi-Λ hypernuclei with a ^{8}Be core using the SkI4 interaction.

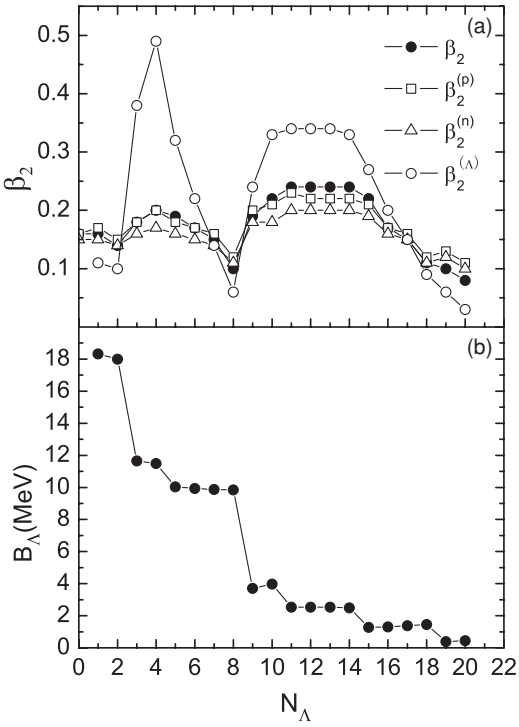

FIG. 8. Same as described in the caption to Fig. 7 but for a ^{50}V core.

Λ binding energies of the spherical hypernucleus become $B_\Lambda = 7.53, 7.47, 7.50$ MeV. Although the deformations lower the binding energies of both the core and hypernuclei, the differences of the two binding energies are smaller by about 0.5 MeV for the results of DSHF, because the deformations of hypernuclei are slightly smaller than of their core nuclei in the case of Be isotopes.

Figures 2–6 show the binding energy surfaces for the core nuclei ^{7,8,9}Be, ^{8,9,10}B, ^{11,12}C, ^{27}Si, and ^{50}V and the corresponding hypernuclei with the SkI4 and SGII forces. Comparing Figs. 2 and 3 it is seen that the two interactions give almost equivalent results apart from a global shift of the energies. One notes in these figures that the ground state of ^{7}Be has the quantum number $K^\pi = n\frac{1}{2}^-$, whereas $K^\pi = n\frac{3}{2}^-$ for ^{9}Be. All the core nuclei ^{7,8,9}Be have large prolate deformations, especially ^{8}Be as we discussed above. The corresponding hypernuclei have similar shapes for the ground states. We can see the same phenomena in Fig. 4: the ground states of ^{8,9,10}B and the corresponding hypernuclei are prolate with little difference of the deformation parameter β.

We notice in Fig. 5 that the shapes of the ground states of ^{11,12}C show oblate deformations, being different from those of ^{7,8,9}Be and ^{8,9,10}B, and the corresponding hypernuclei have also similar oblate deformations. Our calculations predict that the ground states of ^{9}Be and ^{10}B are prolate, while ^{11}C is oblate. These results are consistent with the experimental data of the Q-moments of these nuclei [22]. It was pointed out in Ref. [21] that the deformation plays a very important role for the nonmesonic decay of light hypernuclei. The behavior of the nonmesonic decay rates for the two hypernuclei $^{9}_{\Lambda}$Be and $^{12}_{\Lambda}$C, whose core nuclei are known to be largely deformed, deviates in opposite directions from the prediction of the spherical limit due to the different shapes. Figure 6 indicates that the ground state of ^{27}Si is oblate with $K^\pi = n\frac{1}{2}^+$, whereas ^{50}V is prolate with $p\frac{3}{2}^- \otimes n\frac{7}{2}^-$. The corresponding hypernuclei have similar deformations with the same sign as the core nuclei.

Tables I and II contain the numerical values of the deformation parameters $\beta_2^{(q)}$, binding energies E and B_Λ, and rms radii r_q for the core and hypernuclei in Figs. 2–6. The results of some medium and heavy core and hypernuclei are also tabulated. We find in general that the calculated Λ binding energies agree with the experimental values within about 10% of accuracy. The calculated results of heavy hypernuclei show systematic underbinding compared with the experimental data. The hyperon observables hardly depend on the nuclear Skyrme force chosen for the calculation, but the deformation reduces the Λ binding energy by a few percentages compared to the nondeformed results (B_Λ values given in brackets) in some light nuclei.

The deformations of the single-Λ hypernuclei are always smaller than those of the corresponding core nuclei. To study this aspect in more detail, we display in Figs. 7 and 8 the deformations of hypothetical multihypernuclei $^{n+8}_{n\Lambda}$Be and $^{n+50}_{n\Lambda}$V and the binding energies of the last Λ hyperon up to their Λ driplines. The formation of Ξ hyperons is not considered in these calculations. In the case of the ^{8}Be core, the deformation of the $N_\Lambda = 1, 2$ hypernucleus is always smaller than that of the core nucleus, as also shown in Tables I and II. It is interesting to notice that the deformation difference between

TABLE I. Deformations, energies (in MeV), and radii (in fm) of different (hyper-)nuclei obtained with the Skyrme interaction SkI4. The B_Λ values in brackets are the results of the spherical HF calculations without deformations. Experimental data for B_Λ are from Refs. [3–5].

	K^π	β_2	$\beta_2^{(p)}$	$\beta_2^{(n)}$	$\beta_2^{(\Lambda)}$	$-E$	B_Λ	B_Λ(exp.)	r_p	r_n	r_Λ
^{7}Be	$n\frac{1}{2}^-$	0.52	0.53	0.50		40.36			2.49	2.24	
	$n\frac{3}{2}^-$	−0.15	−0.13	−0.18		39.54			2.40	2.15	
$^{8}_{\Lambda}$Be	$n\frac{1}{2}^- \otimes \Lambda\frac{1}{2}^+$	0.46	0.49	0.47	0.23	46.79	6.43		2.44	2.22	2.20
	$n\frac{3}{2}^- \otimes \Lambda\frac{1}{2}^+$	−0.17	−0.16	−0.20	−0.09	46.22	6.68(6.73)	6.84 ± 0.05 [3]	2.37	2.15	2.26
^{8}Be	0^+	0.63	0.63	0.63		52.76			2.47	2.46	
$^{9}_{\Lambda}$Be	$0^+ \otimes \Lambda\frac{1}{2}^+$	0.59	0.62	0.62	0.34	59.72	6.96(7.47)	6.71 ± 0.04 [3], 5.99 ± 0.07 [5]	2.45	2.45	2.30
$^{10}_{\Lambda\Lambda}$Be	$0^+ \otimes \Lambda 0^+$	0.55	0.60	0.60	0.31	66.56			2.41	2.43	2.31
^{9}Be	$n\frac{3}{2}^-$	0.46	0.53	0.41		59.48			2.37	2.49	
	$n\frac{1}{2}^-$	−0.16	−0.16	−0.16		58.32			2.26	2.40	
$^{10}_{\Lambda}$Be	$n\frac{3}{2}^- \otimes \Lambda\frac{1}{2}^+$	0.43	0.52	0.40	0.25	67.34	7.86		2.36	2.48	2.27
	$n\frac{1}{2}^- \otimes \Lambda\frac{1}{2}^+$	−0.13	−0.13	−0.14	−0.07	66.43	8.11(8.16)	9.11 ± 0.22 [3]	2.25	2.39	2.20
^{8}B	$p\frac{3}{2}^- \otimes n\frac{1}{2}^-$	0.33	0.30	0.39		42.34			2.58	2.18	
	$p\frac{1}{2}^- \otimes n\frac{3}{2}^-$	−0.20	−0.19	−0.22		41.63			2.55	2.15	
$^{9}_{\Lambda}$B	$p\frac{3}{2}^- \otimes n\frac{1}{2}^- \otimes \Lambda\frac{1}{2}^+$	0.30	0.29	0.36	0.16	50.11	7.77		2.52	2.17	2.17
	$p\frac{1}{2}^- \otimes n\frac{3}{2}^- \otimes \Lambda\frac{1}{2}^+$	−0.17	−0.17	−0.20	−0.09	49.46	7.83(7.90)	8.29 ± 0.18 [3]	2.50	2.13	2.15
^{9}B	$p\frac{3}{2}^-$	0.46	0.41	0.53		57.54			2.51	2.37	
	$p\frac{1}{2}^-$	−0.16	−0.16	−0.16		56.36			2.42	2.26	
$^{10}_{\Lambda}$B	$p\frac{3}{2}^- \otimes \Lambda\frac{1}{2}^+$	0.44	0.40	0.52	0.25	65.78	8.24		2.48	2.36	2.24
	$p\frac{1}{2}^- \otimes \Lambda\frac{1}{2}^+$	−0.13	−0.14	−0.13	−0.07	64.89	8.53(8.56)	8.89 ± 0.12 [3], 8.1 ± 0.1 [5]	2.39	2.25	2.17
^{10}B	$p\frac{3}{2}^- \otimes n\frac{3}{2}^-$	0.30	0.30	0.30		69.18			2.40	2.38	
	$p\frac{1}{2}^- \otimes n\frac{1}{2}^-$	−0.20	−0.20	−0.20		68.49			2.37	2.36	
$^{11}_{\Lambda}$B	$p\frac{3}{2}^- \otimes n\frac{3}{2}^- \otimes \Lambda\frac{1}{2}^+$	0.28	0.30	0.29	0.16	78.20	9.02		2.38	2.38	2.22
	$p\frac{1}{2}^- \otimes n\frac{3}{2}^- \otimes \Lambda\frac{1}{2}^+$	−0.18	−0.18	−0.18	−0.10	77.59	9.10(9.17)	10.24 ± 0.05 [3]	2.35	2.35	2.20
^{11}C	$n\frac{1}{2}^-$	−0.30	−0.30	−0.31		72.56			2.57	2.45	
	$n\frac{3}{2}^-$	0.26	0.23	0.30		71.86			2.54	2.42	
$^{12}_{\Lambda}$C	$n\frac{1}{2}^- \otimes \Lambda\frac{1}{2}^+$	−0.29	−0.29	−0.30	−0.17	82.36	9.80		2.54	2.44	2.26
	$n\frac{3}{2}^- \otimes \Lambda\frac{1}{2}^+$	0.24	0.22	0.28	0.14	81.77	9.91(10.06)	10.76 ± 0.19 [3]	2.51	2.41	2.24
^{12}C	0^+	−0.31	−0.31	−0.31		87.55			2.54	2.52	
$^{13}_{\Lambda}$C	$0^+ \otimes \Lambda\frac{1}{2}^+$	−0.29	−0.30	−0.30	−0.17	97.74	10.19(10.52)	11.69 ± 0.12 [3], 11.38 ± 0.05 [5]	2.51	2.51	2.29
^{27}Si	$n\frac{1}{2}^+$	−0.23	−0.23	−0.23		226.43			3.03	2.96	
	$n\frac{3}{2}^+$	−0.28	−0.28	−0.28		226.10			3.04	2.96	
	$n\frac{5}{2}^+$	0.18	0.17	0.20		225.78			3.00	2.94	
$^{28}_{\Lambda}$Si	$n\frac{1}{2}^+ \otimes \Lambda\frac{1}{2}^+$	−0.24	−0.24	−0.24	−0.15	242.10	15.67		3.03	2.96	2.54
	$n\frac{3}{2}^+ \otimes \Lambda\frac{1}{2}^+$	−0.24	−0.24	−0.24	−0.25	241.72	15.62		3.03	2.97	2.54
	$n\frac{5}{2}^+ \otimes \Lambda\frac{1}{2}^+$	0.19	0.18	0.21	0.12	241.51	15.72(15.80)	16.6 ± 0.2 [4,5]	3.00	2.94	2.54
^{50}V	$p\frac{3}{2}^- \otimes n\frac{7}{2}^-$	0.16	0.16	0.15		445.14			3.51	3.58	
	$p\frac{1}{2}^- \otimes n\frac{7}{2}^-$	0.12	0.12	0.12		444.90			3.54	3.58	
	$p\frac{3}{2}^- \otimes n\frac{1}{2}^-$	0.25	0.24	0.25		443.85			3.54	3.63	

TABLE I. *(Continued.)*

	K^π	β_2	$\beta_2^{(p)}$	$\beta_2^{(n)}$	$\beta_2^{(\Lambda)}$	$-E$	B_Λ	B_Λ(exp.)	r_p	r_n	r_Λ
${}^{51}_{\Lambda}$V	$p\frac{3}{2}^- \otimes n\frac{7}{2}^- \otimes \Lambda\frac{1}{2}^+$	0.17	0.16	0.11	0.15	463.47	18.33(18.35)	19.97 ± 0.13 [5]	3.50	3.58	2.91
	$p\frac{1}{2}^- \otimes n\frac{7}{2}^- \otimes \Lambda\frac{1}{2}^+$	0.12	0.12	0.12	0.11	463.23	18.33		3.49	3.58	2.91
	$p\frac{3}{2}^- \otimes n\frac{1}{2}^- \otimes \Lambda\frac{1}{2}^+$	0.23	0.23	0.24	0.15	462.10	18.25		3.53	3.62	2.92
^{88}Y	$p\frac{1}{2}^- \otimes n\frac{9}{2}^+$	0	0	0		774.22			4.13	4.25	
${}^{89}_{\Lambda}$Y	$p\frac{1}{2}^- \otimes n\frac{9}{2}^+ \otimes \Lambda\frac{1}{2}^+$	0	0	0	0	794.95	20.73	22.0 ± 0.5 [4], 23.1 ± 0.5 [5]	4.13	4.25	3.34
^{207}Pb	$n\frac{1}{2}^-$	0	0	0		1644.7			5.42	5.59	
${}^{208}_{\Lambda}$Pb	$n\frac{1}{2}^- \otimes \Lambda\frac{1}{2}^+$	0	0	0	0	1667.2	22.41	26.5 ± 0.5 [4], 26.3 ± 0.8 [5]	5.41	5.59	4.21

the core and the corresponding hypernuclei is large in the cases of $N_\Lambda = 1$ and 2, whereas the two deformations are very similar in the cases of $N_\Lambda = 3$ and 4, close to the Λ drip line. At the same time, the Λ separation energy is large in the cases of $N_\Lambda = 1$ and 2, whereas it is almost zero for the $N_\Lambda = 3, 4$ hypernuclei.

The general trend of hypernuclei of ^{50}V is quite different. The deformations of the hypernuclei are larger than those of the core, especially at the middle of the shells specified by $N_\Lambda = 8$ and 20. In particular, we observe a pronounced variation of the Λ and core deformations and the Λ binding energies as a function of N_Λ. This evolution of the deformations

TABLE II. Same as Table I with the Skyrme interaction SGII.

	K^π	β_2	$\beta_2^{(p)}$	$\beta_2^{(n)}$	$\beta_2^{(\Lambda)}$	$-E$	B_Λ	B_Λ(exp.)	r_p	r_n	r_Λ
^{7}Be	$n\frac{1}{2}^-$	0.47	0.47	0.46		44.0			2.42	2.24	
	$n\frac{3}{2}^-$	−0.16	−0.13	−0.19		43.56			2.33	2.15	
${}^{8}_{\Lambda}$Be	$n\frac{1}{2}^- \otimes \Lambda\frac{1}{2}^+$	0.34	0.36	0.38	0.17	50.68	6.68		2.33	2.21	2.15
	$n\frac{3}{2}^- \otimes \Lambda\frac{1}{2}^+$	−0.15	−0.14	−0.19	−0.08	50.43	6.87	6.84 ± 0.05 [3]	2.28	2.16	2.12
^{8}Be	0^+	0.64	0.64	0.64		55.81			2.48	2.47	
${}^{9}_{\Lambda}$Be	$0^+ \otimes \Lambda\frac{1}{2}^+$	0.59	0.62	0.61	0.33	62.87	7.06	6.71 ± 0.04 [3], 5.99 ± 0.07 [5]	2.43	2.45	2.29
${}^{10}_{\Lambda\Lambda}$Be	$0^+ \otimes \Lambda 0^+$	0.55	0.60	0.60	0.32	69.69			2.39	2.44	2.30
^{9}Be	$n\frac{3}{2}^-$	0.46	0.53	0.41		63.35			2.39	2.45	
	$n\frac{1}{2}^-$	−0.15	−0.14	−0.15		62.69			2.27	2.35	
${}^{10}_{\Lambda}$Be	$n\frac{3}{2}^- \otimes \Lambda\frac{1}{2}^+$	0.38	0.45	0.36	0.21	71.26	7.91		2.34	2.42	2.24
	$n\frac{1}{2}^- \otimes \Lambda\frac{1}{2}^+$	−0.13	−0.13	−0.14	−0.07	70.81	8.12	9.11 ± 0.22 [3]	2.25	2.39	2.20
^{8}B	$p\frac{3}{2}^- \otimes n\frac{1}{2}^-$	0.34	0.32	0.39		47.40			2.47	2.20	
	$p\frac{1}{2}^- \otimes n\frac{3}{2}^-$	−0.19	−0.18	−0.21		46.86			2.43	2.16	
${}^{9}_{\Lambda}$B	$p\frac{3}{2}^- \otimes n\frac{1}{2}^- \otimes \Lambda\frac{1}{2}^+$	0.31	0.30	0.37	0.17	55.62	8.22		2.40	2.20	2.12
	$p\frac{1}{2}^- \otimes n\frac{3}{2}^- \otimes \Lambda\frac{1}{2}^+$	−0.17	−0.17	−0.20	−0.09	55.14	8.28	8.29 ± 0.18 [3]	2.36	2.16	2.10
^{9}B	$p\frac{3}{2}^-$	0.46	0.41	0.53		61.32			2.48	2.38	
	$p\frac{1}{2}^-$	−0.15	−0.15	−0.14		60.63			2.38	2.26	
${}^{10}_{\Lambda}$B	$p\frac{3}{2}^- \otimes \Lambda\frac{1}{2}^+$	0.36	0.34	0.41	0.19	69.75	8.43		2.40	2.33	2.18
	$p\frac{1}{2}^- \otimes \Lambda\frac{1}{2}^+$	−0.14	−0.15	−0.14	−0.08	69.35	8.72	8.89 ± 0.12 [3], 8.1 ± 0.1 [5]	2.34	2.27	2.15

TABLE II. *(Continued.)*

	K^π	β_2	$\beta_2^{(p)}$	$\beta_2^{(n)}$	$\beta_2^{(\Lambda)}$	$-E$	B_Λ	B_Λ(exp.)	r_p	r_n	r_Λ
^{10}B	$p\frac{3}{2}^- \otimes n\frac{3}{2}^-$	0.30	0.30	0.30		72.83			2.39	2.37	
	$p\frac{1}{2}^- \otimes n\frac{1}{2}^-$	−0.17	−0.17	−0.17		72.31			2.36	2.34	
$^{11}_{\Lambda}$B	$p\frac{3}{2}^- \otimes n\frac{3}{2}^- \otimes \Lambda\frac{1}{2}^+$	0.29	0.30	0.30	0.16	81.87	9.04		2.37	2.38	2.21
	$p\frac{1}{2}^- \otimes n\frac{3}{2}^- \otimes \Lambda\frac{1}{2}^+$	−0.18	−0.18	−0.18	−0.10	81.45	9.14	10.24 ± 0.05 [3]	2.34	2.35	2.20
^{11}C	$n\frac{1}{2}^-$	−0.31	−0.30	−0.31		77.07			2.55	2.45	
	$n\frac{3}{2}^-$	0.26	0.23	0.30		76.53			2.51	2.42	
$^{12}_{\Lambda}$C	$n\frac{1}{2}^- \otimes \Lambda\frac{1}{2}^+$	−0.29	−0.29	−0.30	−0.17	86.95	9.88		2.51	2.45	2.25
	$n\frac{3}{2}^- \otimes \Lambda\frac{1}{2}^+$	0.21	0.18	0.25	0.11	86.54	10.01	10.76 ± 0.19 [3]	2.46	2.41	2.22
^{12}C	0^+	−0.31	−0.31	−0.31		91.48			2.54	2.52	
$^{13}_{\Lambda}$C	$0^+ \otimes \Lambda\frac{1}{2}^+$	−0.29	−0.30	−0.30	−0.17	101.70	10.22	11.69 ± 0.12 [3], 11.38 ± 0.05 [5]	2.51	2.51	2.29
^{27}Si	$n\frac{1}{2}^+$	−0.27	−0.28	−0.27		230.19			3.07	2.99	
	$n\frac{3}{2}^+$	−0.28	−0.28	−0.27		229.96			3.07	2.99	
	$n\frac{5}{2}^+$	0.18	0.17	0.20		229.26			3.02	2.95	
$^{28}_{\Lambda}$Si	$n\frac{1}{2}^+ \otimes \Lambda\frac{1}{2}^+$	−0.24	−0.24	−0.24	−0.15	245.77	15.58		3.03	2.97	2.54
	$n\frac{3}{2}^+ \otimes \Lambda\frac{1}{2}^+$	−0.28	−0.29	−0.28	−0.18	245.48	15.52		3.06	3.00	2.56
	$n\frac{5}{2}^+ \otimes \Lambda\frac{1}{2}^+$	0.19	0.18	0.21	0.12	245.0	15.74	16.6 ± 0.2 [4,5]	3.00	2.95	2.54
^{50}V	$p\frac{3}{2}^- \otimes n\frac{7}{2}^-$	0.15	0.15	0.14		450.26			3.54	3.57	
	$p\frac{1}{2}^- \otimes n\frac{7}{2}^-$	0.10	0.09	0.10		450.08			3.53	3.56	
	$p\frac{3}{2}^- \otimes n\frac{1}{2}^-$	0.24	0.24	0.24		449.31			3.58	3.63	
$^{51}_{\Lambda}$V	$p\frac{3}{2}^- \otimes n\frac{7}{2}^- \otimes \Lambda\frac{1}{2}^+$	0.15	0.15	0.15	0.10	468.51	18.25	19.97 ± 0.13 [5]	3.53	3.57	2.92
	$p\frac{1}{2}^- \otimes n\frac{7}{2}^- \otimes \Lambda\frac{1}{2}^+$	0.10	0.10	0.10	0.07	468.34	18.26		3.52	3.56	2.92
	$p\frac{3}{2}^- \otimes n\frac{1}{2}^- \otimes \Lambda\frac{1}{2}^+$	0.24	0.24	0.24	0.16	467.50	18.19		3.56	3.61	2.93
^{88}Y	$p\frac{1}{2}^- \otimes n\frac{9}{2}^+$	0	0	0		781.83			4.17	4.23	
$^{89}_{\Lambda}$Y	$p\frac{1}{2}^- \otimes n\frac{9}{2}^+ \otimes \Lambda\frac{1}{2}^+$	0	0	0	0	802.12	20.29	22.0 ± 0.5 [4], 23.1 ± 0.5 [5]	4.17	4.23	3.34
^{207}Pb	$n\frac{1}{2}^-$	0	0	0		1655.2			5.45	5.58	
$^{208}_{\Lambda}$Pb	$n\frac{1}{2}^- \otimes \Lambda\frac{1}{2}^-$	0	0	0	0	1677.6	22.39	26.5 ± 0.5 [4], 26.3 ± 0.8 [5]	5.45	5.58	4.22

is determined by the competition between the deformation-driving particle-vibration coupling and the pairing correlations restoring the spherical symmetry of the nuclear system. Therefore the shell structure of nuclei gives rise to a variety of different shapes, i.e., prolate, oblate, and triaxial, depending on the position of the Fermi energy between two closed shells. In the hyperon case, because of no pairing, the deformations are only determined by the particle-vibration coupling, and become very large between two closed shells.

IV. SUMMARY

In summary, we studied deformations of core and hypernuclei in a broad region of the mass table by using an extended DSHF formalism. To this purpose we introduced the microscopic ΛN interaction of Refs. [17,18] extended to isospin-asymmetric matter, together with nuclear pairing correlations and three different nucleonic Skyrme forces which have been tested for deformed pf-shell and d-shell core nuclei.

We found that the calculated large prolate deformations of the p-shell nuclei ^{9}Be and ^{10}B are confirmed by the experimental data of Q moments, while the large oblate deformation of ^{11}C are found both in the experiment and the calculations. The calculated core nuclei and the corresponding hypernuclei have similar deformations with the same sign, which agree with the calculations of the α-cluster model in Ref. [2]. The obtained Λ binding energies B_Λ confront satisfactorily with

experimental values, which leaves little room for additional contributions to our effective ΛN interaction due to hyperonic three-body forces or finite-size corrections. A proper treatment of deformations is important in the future study of hypernuclei not only regarding the binding energies of hypernuclei B_Λ and $B_{\Lambda\Lambda}$, but also other properties like the fine structure and the nonmesonic decays of hypernuclei.

ACKNOWLEDGMENTS

We thank J. C. Pei for stimulating discussions. This work was supported by the National Science Foundation of China under contract nos. 10605018 and 10575036, CAS-KJCX-SYW-N2, and the Program for New Century Excellent Talents in Fujian Province University.

[1] T. Motoba, H. Bandō, K. Ikeda, and T. Yamada, Prog. Theor. Phys. Suppl. **81**, 42 (1985); H. Feshbach, Nucl. Phys. **A507**, 219c (1990); B. F. Gibson and E. V. Hungerford III, Phys. Rep. **257**, 349 (1995).

[2] H. Bandō, T. Motoba, and J. Žofka, Int. J. Mod. Phys. A **5**, 4021 (1990).

[3] D. H. Davis, Nucl. Phys. **A754**, 3 (2005).

[4] T. Hasegawa *et al*., Phys. Rev. C **53**, 1210 (1996); H. Hotchi *et al*., Phys. Rev. C **64**, 044302 (2001).

[5] O. Hashimoto and H. Tamura, Prog. Part. Nucl. Phys. **57**, 564 (2006).

[6] M. Danysz *et al*., Phys. Rev. Lett. **11**, 29 (1963); Nucl. Phys. **49**, 121 (1963); R. H. Dalitz, D. H. Davis, P. H. Fowler, A. Montwill, J. Pniewski, and J. A. Zakrzewski, Proc. R. Soc. London A **426**, 1 (1989).

[7] S. Aoki *et al*., Prog. Theor. Phys. **85**, 1287 (1991).

[8] G. B. Franklin, Nucl. Phys. **A585**, 83c (1995).

[9] H. Takahashi *et al*., Phys. Rev. Lett. **87**, 212502 (2001).

[10] J. Mareš and J. Žofka, Z. Phys. A **333**, 209 (1989); **345**, 47 (1993); M. Rufa, J. Schaffner, J. Maruhn, H. Stöcker, W. Greiner, and P.-G. Reinhard, Phys. Rev. C **42**, 2469 (1990); N. K. Glendenning, D. Von-Eiff, M. Haft, H. Lenske, and M. K. Weigel, *ibid.* **48**, 889 (1993); C. M. Keil, F. Hofmann, and H. Lenske, *ibid.* **61**, 064309 (2000).

[11] H. Shen, F. Yang, and H. Toki, Prog. Theor. Phys. **115**, 325 (2006).

[12] J. Schaffner, C. Greiner, and H. Stöcker, Phys. Rev. C **46**, 322 (1992); J. Schaffner, C. B. Dover, A. Gal, C. Greiner, D. J. Millener, and H. Stöcker, Ann. Phys. (NY) **235**, 35 (1994); J. Schaffner-Bielich and A. Gal, Phys. Rev. C **62**, 034311 (2000).

[13] M. Rayet, Ann. Phys. (NY) **102**, 226 (1976); Nucl. Phys. **A367**, 381 (1981).

[14] D. J. Millener, C. B. Dover, and A. Gal, Phys. Rev. C **38**, 2700 (1988).

[15] Y. Yamamoto, H. Bandō, and J. Žofka, Prog. Theor. Phys. **80**, 757 (1988); Y. Yamamoto and H. Bandō, *ibid.* **83**, 254 (1990); D. Halderson, Phys. Rev. C **48**, 581 (1993); **C61**, 034001 (2000); J. Hao, T. T. S. Kuo, A. Reuber, K. Holinde, J. Speth, and D. J. Millener, Phys. Rev. Lett. **71**, 1498 (1993); **74**, 004762 (1995); Y. Yamamoto, T. Motoba, H. Himeno, K. Ikeda, and S. Nagata, Prog. Theor. Phys. Suppl. **117**, 361 (1994); I. Vidaña, A. Polls, A. Ramos, and M. Hjorth-Jensen, Nucl. Phys. **A644**, 201 (1998); Y. Tzeng, S. Y. T. Tzeng, T. T. S. Kuo, and T.-S. H. Lee, Phys. Rev. C **60**, 044305 (1999); D. J. Millener, Nucl. Phys. **A691**, 93 (2001); S. Fujii, R. Okamoto, and K. Suzuki, Phys. Rev. C **66**, 054301 (2002).

[16] D. E. Lanskoy and Y. Yamamoto, Phys. Rev. C **55**, 2330 (1997).

[17] J. Cugnon, A. Lejeune, and H.-J. Schulze, Phys. Rev. C **62**, 064308 (2000).

[18] I. Vidaña, A. Polls, A. Ramos, and H.-J. Schulze, Phys. Rev. C **64**, 044301 (2001).

[19] H.-J. Schulze, A. Lejeune, J. Cugnon, M. Baldo, and U. Lombardo, Phys. Lett. **B355**, 21 (1995); M. Baldo, G. F. Burgio, H. J. Schulze, Phys. Rev. C **57**, 704 (1998); Phys. Rev. C **61**, 055801 (2000); H.-J. Schulze, A. Polls, A. Ramos, and I. Vidaña, Phys. Rev. C **73**, 058801 (2006).

[20] T. H. Ho and A. B. Volkov, Phys. Lett. **B30**, 303 (1969); J. Žofka, Czech. J. Phys. **B30**, 95 (1980); W. H. Bassichis and A. Gal, Phys. Rev. C **1**, 28 (1970).

[21] K. Hagino and A. Parreño, Phys. Rev. C **63**, 044318 (2001).

[22] F. Ajzenberg-Selove, Nucl. Phys. **A490**, 1 (1988); **A506**, 1 (1990).

[23] K. Hara and Y. Sun, Int. J. Mod. Phys. E **4**, 637 (1995).

[24] D. Vautherin, Phys. Rev. C **7**, 296 (1973).

[25] C. Gustafsson, I. L. Lamm, B. Nilsson, and S. G. Nilsson, Ark. Fys. **36**, 613 (1967).

[26] P. Ring and P. Schuck, *The Nuclear Many-Body Problem* (Springer-Verlag, Berlin, 1980).

[27] H. Sagawa, X.-R. Zhou, X. Z. Zhang, and T. Suzuki, Phys. Rev. C **70**, 054316 (2004); **72**, 054311 (2005).

[28] P. M. M. Maessen, Th. A. Rijken, and J. J. de Swart, Phys. Rev. C **40**, 2226 (1989).

[29] R. B. Wiringa, V. G. J. Stoks, and R. Schiavilla, Phys. Rev. C **51**, 38 (1995).

[30] V. Blum, G. Lauritsch, J. A. Maruhn, and P.-G. Reinhard, J. Comput. Phys. **100**, 364 (1992).

[31] M. Bender, K. Rutz, P.-G. Reinhard, J. A. Maruhn, and W. Greiner, Phys. Rev. C **60**, 034304 (1999).

[32] N. Tajima, P. Bonche, H. Flocard, P.-H. Heenen, and M. S. Weiss, Nucl. Phys. **A551**, 434 (1993).

[33] H. Sagawa, T. Suzuki, and K. Hagino, in *Proceedings of the International Symposium on Frontiers of Collective Motions* (CM2002) (World Scientific, Singapore, 2003), p. 236; H. Sagawa, T. Suzuki, and K. Hagino, Nucl. Phys. **A722**, C183 (2003); Phys. Rev. C **68**, 014317 (2003).

[34] M. Bender, K. Rutz, P.-G. Reinhard, and J. A. Maruhn, Eur. Phys. J. A **8**, 59 (2000).

[35] S. Ajimura *et al*., Phys. Rev. Lett. **86**, 4255 (2001); H. Akikawa *et al*., Phys. Rev. Lett. **88**, 082501 (2002).

[36] I. Vidaña, A. Ramos, and A. Polls, Phys. Rev. C **70**, 024306 (2004).